

## UV-Blocking Property of Dumbbell-Shaped ZnO Crystallites on Cotton Fabrics

R. H. Wang,\* J. H. Xin,\* and X. M. Tao

Nanotechnology Center for Functional and Intelligent Textiles and Apparel, Institute of Textiles &amp; Clothing, The Hong Kong Polytechnic University, Hung Hom, Kowloon, Hong Kong

Received March 2, 2005

A facile process to prepare uniform dumbbell-shaped ZnO crystallites was presented. The evidence in this Article discovered a unique morphological effect on the UV-blocking property. The as-prepared ZnO crystallites were characterized by XRD, HRTEM, FESEM, UV-blocking, and Raman scattering spectra. Our tentative investigation created a breakthrough to both the ultrahigh “Ultraviolet protection factor” (UPF) and the overall-range of complete UV-radiation blocking. Therefore, the as-prepared structural material demonstrated a significant advance in protective functional treatment and provided a potential commercialization.

## Introduction

The synthesis of one-dimensional (1-D) nano- or micro-structured ZnO semiconductor materials ranging from wires,<sup>1</sup> belts,<sup>2</sup> branches,<sup>3</sup> needles,<sup>4</sup> towers,<sup>5</sup> tubes,<sup>6</sup> columns,<sup>7</sup> tetrapods,<sup>8</sup> nails,<sup>9</sup> helices,<sup>10</sup> combs,<sup>11</sup> and tadpoles<sup>12</sup> to dumbbells<sup>13</sup> has attracted considerable research activity because of their great potential for fundamental studies of the roles of dimensionality and size in their physical properties as well

as for applications in optoelectronic devices and functional materials. Hydrothermal methods<sup>14</sup> are recognized as excellent procedures for the preparation of 1-D ZnO nano-crystallites, as the resulting particles have narrow size distribution, good crystallization, and high-quality growth orientation. For application at ambient pressure, nevertheless, hydrothermal reaction is not suitable for larger scale and industrial preparation because of pressure limitation. To recap this, we previously developed an ambient-pressure and low-temperature zero-gel-seeded opening crystallization (APLTZOC) approach.<sup>13a</sup> It provided a rational route to scale-up the preparation of 1-D ZnO nano- and microstructured materials, as part of a program to develop routes to nano- and microscale ZnO materials on cotton fabrics with better UV-blocking property.

Designing and modifying fabrics in such a way that they offer high protection against UV radiation (UV-R, both UVA and UVB, falls into the regions of 315–400 and 280–315 nm, respectively, of the solar spectra) is a relatively new application.<sup>15d</sup> To indicate the protection from UV-R, the term “sun protection factors” (SPFs) is widely used; it is usually associated with cosmetic skin protection products and was first established in Australia and New Zealand. The category can now be applied to textiles and identified on

\* To whom correspondence should be addressed. Tel: +852-2766-6474. Fax: +852-2773-1432. E-mail: tcroger.rhwang@polyu.edu.hk (R.H.W.); tcxinh@inet.polyu.edu.hk (J.H.X.).

- (1) (a) Huang, M. H.; Mao, S.; Feick, H.; Yan, H.; Wu, Y.; Kind, H.; Weber, E.; Russo, R.; Yang, P. *Science* **2001**, *292*, 1897–1899. (b) Greene, L. E.; Law, M.; Goldberger, J.; Kim, F.; Johnson, J. C.; Zhang, Y.; Saykally, R. J.; Yang, P. *Angew. Chem., Int. Ed.* **2003**, *42*, 3031–3034.
- (2) Pan, Z. W.; Dai, Z. R.; Wang, Z. L. *Science* **2001**, *291*, 1947–1949.
- (3) Milliron, D. J.; Hughes, S. T.; Cui, Y.; Manna, L.; Li, J.; Wang, L. W.; Alivisatos, A. P. *Nature* **2004**, *430*, 190–195.
- (4) Ledwith, D.; Pillai, S. C.; Watson, G. W.; Kelly, J. M. *Chem. Commun.* **2004**, 2294–2295.
- (5) Hu, P.; Liu, Y.; Wang, X.; Fu, L.; Zhu, D. *Chem. Commun.* **2004**, 1304–1305.
- (6) Zhang, J.; Sun, L.; Liao, C.; Yan, C. *Chem. Commun.* **2002**, 262–263.
- (7) Tian, Z. R.; Voigt, J. A.; Liu, J.; McKenzie, B.; Mcdermott, M. J. *J. Am. Chem. Soc.* **2002**, *124*, 12954–12955.
- (8) Zhang, Y.; Jia, H.; Luo, X.; Chen, X.; Yu, D.; Wang, R. *J. Phys. Chem. B* **2003**, *107*, 8289–8293.
- (9) Lao, J. Y.; Huang, J. Y.; Wang, D. Z.; Ren, Z. F. *Nano Lett.* **2003**, *3*, 235–238.
- (10) Kong, X. Y.; Wang, Z. L. *Nano Lett.* **2003**, *3*, 1625–1631.
- (11) Yan, H.; He, R.; Johnson, J.; Law, M.; Saykally, R. J.; Yang, P. *J. Am. Chem. Soc.* **2003**, *125*, 4728–4729.
- (12) Gao, P.; Wang, Z. L. *J. Phys. Chem. B* **2002**, *106*, 12653–12658.
- (13) (a) Wang, R. H.; Xin, J. H.; Tao, X. M.; Daoud, W. A. *Chem. Phys. Lett.* **2004**, *398*, 250–255. (b) Wang, B. G.; Shi, E. W.; Zhong, W. Z. *Cryst. Res. Technol.* **1998**, *33*, 937–941.

- (14) (a) Vayssieres, L. *Adv. Mater.* **2003**, *15*, 464–466. (b) Vayssieres, L.; Keis, K.; Lindquist, S.-E.; Hagfeldt, A. *J. Phys. Chem. B* **2001**, *105*, 3350–3352.
- (15) (a) Peplow, M. *Nature* **2004**, *429*, 620. (b) Daoud, W. A.; Xin, J. H. *J. Am. Ceram. Soc.* **2004**, *87*, 953–955. (c) Daoud, W. A.; Xin, J. H. *J. Sol-Gel Sci. Technol.* **2004**, *29*, 25–29. (d) Xin, J. H.; Daoud, W. A.; Kong, Y. Y. *Text. Res. J.* **2004**, *74*, 97–100.

the product labeling. SPF is a measure of how much a sunscreen protects the skin from burning, and it is measured by timing how long skin covered with sunscreen takes to burn compared with unprotected skin. The detailed testing procedure based on an in-vivo method is given in an Australian/New Zealand standard AS/NZS 2604. The other term "Ultraviolet protection factor" (UPF) defined in Australian/New Zealand standard AS/NZS 4399: 1996 (Appendix: solar spectral irradiance used was measured at noon on 17 January 1990 for Melbourne (38 °C)) has now been widely adopted by the textile and clothing industry worldwide. UPF ratings indicate how much the material reduces UV exposure. For example, a rating of 15 indicates that 1/15th of the hazardous UV rays falling on the surface will pass through and that the skin's exposure will thus be reduced by a factor of 15. UPF is based on an in-vitro one, and it is a ranking of the sun-protective abilities of a textile. It is the ratio of the average effective ultraviolet UV-R irradiation calculated for unprotected skin to the average effective UV-R irradiation calculated for skin protected by the test fabric. The UPF of a fabric depends on fiber content and weave, fabric color, finishing processes, the presence of additives, and laundering. Based on these criteria, the minimum UPF for clothing should be 40 to 50. The UPF rating of less than 15, between 15 and 50, and more than 50 (50+) are generally classified as nonrateable, good, and excellent UV-blocking properties for fabrics, respectively. A low UPF (less than 15) of cotton is inadequate protection for outdoor wearers; therefore, clothing with a greater UPF should be worn. The sun protection of fabrics can be increased in various ways, including the use of UV-protection additives,<sup>16</sup> thin films of sol-gel processed titania,<sup>15</sup> or ZnO nanosols/nanorods.<sup>13a</sup> The washfastness of those additives was limited.<sup>16</sup> However, excellent washfastness after 55 home launderings (the UV-blocking range is 332–280 nm and UPF rating is 50+) was achieved as a thin layer of titania was formed on the cotton fabrics.<sup>15</sup> It still remains a challenge to achieve complete UV-blocking. In our previous report, we found ZnO nanorods (the UV-blocking range is 375–280 nm) had the potential to block a 53-nm-wider range of UV-R than that of titania thin films. The exciting phenomenon might stimulate promising applications in cosmetic, textiles, and outdoor shelters.

In this Article, the morphological effect on the UV-blocking property was mainly investigated. The dumbbell-shaped ZnO was prepared with the aid of ZnO nanorods, and the unique ultrahigh UPF has been achieved. In contrary to one-dimensional nanostructures, dumbbell-shaped morphology is less known. The mechanism might be due to the coupling of nanorods. Our tentative investigation created a breakthrough to both the ultrahigh UPF and the overall-range of complete UV-radiation blocking. Therefore, the as-prepared structural material demonstrated a significant advance in protective functional treatment and provided a potential commercialization.

## Experimental Section

All chemicals were used as-received. The substrates (knitted or woven cotton fabrics) were scoured by nonionic detergent to remove the wax, grease, and other finishing chemicals from fabrics before coating. The scouring process was performed at 80 °C for 30 min.

**Synthesis of 3 wt % ZnO Nanosol.** The synthesis art of ZnO sol is different from the method reported in the literature.<sup>1b</sup> The detailed method is as follows. An amount of 24.4 g of zinc acetate dihydrate ( $\text{ZnAc}\cdot 2\text{H}_2\text{O}$ , International Laboratory, USA) was added to 200 mL of 2-methoxyethanol (EGME, International Laboratory, USA) under vigorous stirring at about 105 °C for 30 min. Subsequently, triethenamine (TEA, International Laboratory, USA), with the same molar ratio as  $\text{ZnAc}\cdot 2\text{H}_2\text{O}$  (11.25 g), was added dropwise using a syringe to dissolve  $\text{ZnAc}\cdot 2\text{H}_2\text{O}$  and to form a transparent homogeneous solution; the reaction mixture was stirred at 105 °C for 10 min and then stored seamlessly at ambient temperature overnight. The as-prepared sol was quite sensitive to water.

**Coating Processes.** The as-prepared sol might be applied onto the substrate by various techniques as follows: dip-pad-cure, dip-coating, and spraying processes. In our study, the dip-pad-cure process was employed to form a thick layer of seeds. The cleaned substrates were dipped in the ZnO sol for one minute and then padded with an automatic padder (Rapid Labortex Co., LTD, Taipei, Taiwan) at a nip pressure of 2.75 kg/cm<sup>2</sup>. The padded substrates were air-dried for 30 min and finally cured at 130 °C for 30 min in a preheated curing oven (Memmert ULE800 Universal Oven, Germany) to ensure particle adhesion to the substrate surface. The curing temperature might be varied from room temperature to several hundred degrees.

**Formation of ZnO Nanorods.** The detailed procedures were reported previously.<sup>13a</sup> The seeded substrates were suspended in an open aqueous solution of  $\text{ZnAc}\cdot 2\text{H}_2\text{O}$  (0.025 mol L<sup>-1</sup>) and TEA (0.025 mol L<sup>-1</sup>) at room temperature for a predetermined time from 0.5 to 6 h, depending on the desired nanorod length and morphology. Typically, the ZnO nanorods were 10–50 nm in diameter and 300–500 nm in length. Finally, the samples were rinsed with deionized water to remove any residual salt or amino complex and allowed to dry at 60 °C.

**Synthesis of Dumbbell-Shaped ZnO.** The ZnO nanorods built cotton fabrics were suspended into an aqueous solution of  $\text{ZnAc}\cdot 2\text{H}_2\text{O}$  (0.01 mol L<sup>-1</sup>) and triethenamine (TEA, International Laboratory, USA, 0.01 mol L<sup>-1</sup>) at ambient pressure for 6 h at 95 °C with vigorous stirring. Finally the samples were rinsed with deionized water (self-made) to remove any residual salt or amino complex and allowed to dry at 60 °C.

**Instruments and Characterization.** The products were structurally characterized by powder X-ray diffraction (XRD, Philips X'pert diffractometer in  $\theta$ - $2\theta$  configuration). The morphologies were investigated using field emission scanning electron microscopy (FESEM, Leica Stereo-scan 440, operating at 20 kV; JSM-6335F at 3.0 kV, JEOL, Tokyo, Japan). The lattice space can be determined employing high-resolution transmission electron microscopy (HRTEM, JEOL JEM 2010 operated at 200 kV). UPF was measured by a Varian Cary 300 UV spectrophotometer with the aid of the fibrous cellulose as substrates according to the Australian/New Zealand Standard AS/NZS 4399:1996. Washfastness was evaluated with reference to the Technic Manual of the American Association of Textile Chemists and Colorists (AATCC). Washing was performed using a laundering machine (AATCC Standard Instrumental Atlas Launder-Ometer LEF, Atlas electric devices company, Chicago, USA) at 49 °C in a 1.2 L stainless steel lever

(16) (a) Eckhardt, C.; Rohwer, H. *Text. Chem. Color. Am. Dyest. Rep.* **2000**, 32, 21–23. (b) Hilfiker, R.; Kaufmann, W.; Reinert, G.; Schmidt, E. *Text. Res. J.* **1996**, 66, 61–70. (c) Reinert, G.; Fuso, F.; Hilfiker, R.; Schmidt, E. *Text. Chem. Color.* **1997**, 29, 36–43.

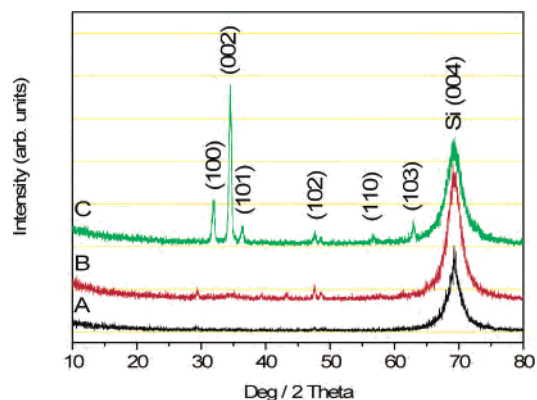


**Figure 1.** A typical indexed X-ray diffraction pattern of the as-prepared products. A: control, B: nanosol, C: dumbbell-shaped ZnO.

lock canister. The substrates were leached in 200 mL of 0.15% aqueous solution of sodium lauryl sulfate (SDS) and in the presence 50 steel balls for 45 min. For easy understanding, this washing procedure is equivalent to 5 cycles of home laundering according to the AATCC Test Method 61-1996 test No. 2A. The substrates were then rinsed intensively with water and dried at room temperature prior to further investigations.

## Results and Discussion

The products were structurally characterized by XRD revealing that dumbbell-shaped ZnO was typical wurtzite structure (Figure 1) corresponding to the Joint Committee on Powder Diffraction Standard (JCPDS) card number-36-1451 (the referenced  $a = 3.24982 \text{ \AA}$ ;  $c = 5.20661 \text{ \AA}$ ), that is, a hexagonal close packing of oxygen and zinc atoms in point group 3m and spacing group  $P6_3mc$  with zinc atoms in tetrahedral sites. Similar to colloidal nanocrystal heterostructures with linear and branched topology,<sup>3</sup> the homostructural fabrication of inorganically coupled colloidal quantum dots and rods, connected epitaxially at dendritic and linear junctions within single nanocrystals, might be achieved with the benefit of poor orientation of ZnO nanorods (Figure 2a) and/or mobile seeds of nanorods removed from the substrate because of mobility of stirred solution. The dendritic structure was flowerlike, consisting of various numbers of bells (Indices in Figure 2b and Figure 2c). The typical dumbbell structure was observed in Figure 2d, 2e, and 2f; the size and dimensionality of this kind of structure might be tuneable by changing the length of the original rods and/or varying the synthesizing time. The as-prepared dumbbells were 500 nm to tens of micrometers in length and with diameters of 200 up to  $1 \mu\text{m}$ . The as-prepared dumbbell-shaped structural products grown after 3 h and 6 h were shown in Figure 2e and 2f, respectively. To further understand the homojunctions, high-resolution transmission electron microscopy (HRTEM, JEOL JEM 2010 operated at 200 kV) was employed, and it revealed that the representative dumbbells had fairly large lattice mismatches at the area indexed using the arrows (Figure 3). The imaging process was carried out using the Fast-Fourier transformation method. The power spectrum shown in the top right corner is in agreement with the diffraction pattern (not shown here). The noise-reduced image of the marked square is shown in

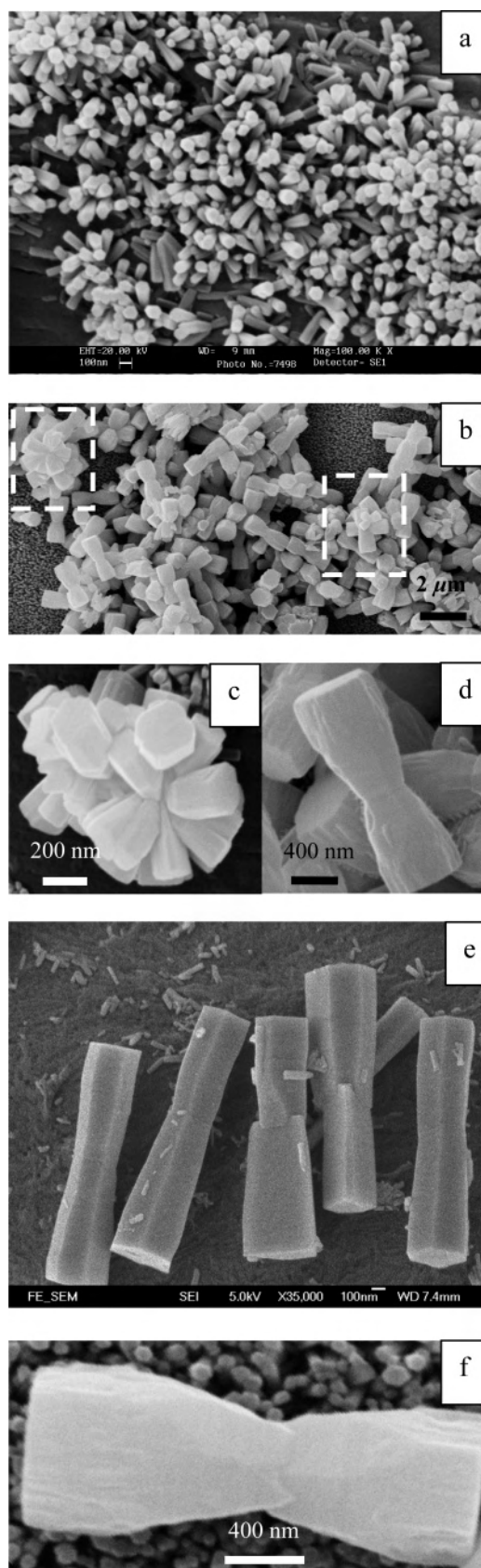


**Figure 2.** (a) A typical SEM image of ZnO nanorods grown on cotton fabrics; (b) a low-magnification SEM image of ZnO microdumbbells and branched structures (rectangles indexed); (c) flower-like dendritic microcrystallites; (d) a high-magnification SEM image of ZnO microdumbbells and an individual ZnO dumbbell shows clear homojunction after 3 h, 6 h; (e) growth based on the coupling of ZnO nanorods, respectively.

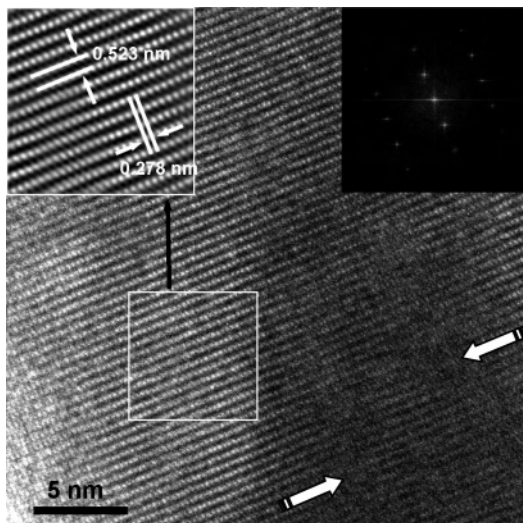


**Figure 3.** A high-resolution TEM image reveals that the dumbbells are highly crystalline, grow along the (001) direction, and have fairly high lattice mismatches (arrows indexed). The imaging process was carried out using the Fast-Fourier transformation method. The noise-reduced image of the marked square is shown in the top left corner. The inset in the top right corner illustrates the power spectrum.

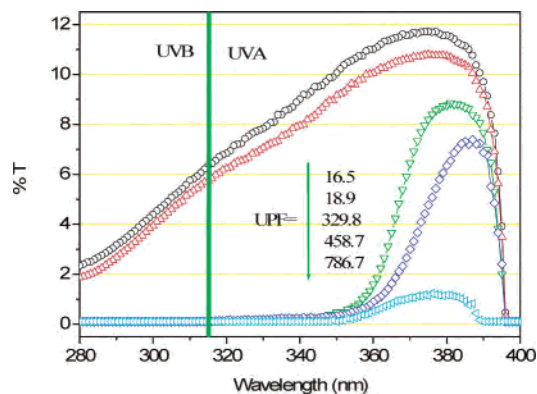


**Figure 4.** The UV-blocking spectra of zinc oxide nanosol-finished woven cotton fabrics. From top to bottom: cotton fabric sample, treated fabric without curing, cured at 130 °C, 150 °C, and 170 °C, respectively.

the top left corner. It shows the lattice fringes of 0.523 and 0.278 nm, corresponding to the (001) and (100) planes of ZnO, respectively.

“Ultraviolet protection factor” (UPF) can directly evaluate the UV-blocking activity of the as-prepared products. The UPF of a fabric depends on various factors, including fiber content, weave, fabric color, finishing processes, the presence of additives, and laundering. In this study, we employed woven cellulosic cotton fabric as substrates. The finishing processes included dip-pad-cure process, nanorods growth, and dumbbell-shaped ZnO growth. To achieve a thicker film, a higher concentration of 3 wt % was used and each sample was finished twice. The fabrics treated using ZnO nanosols were studied as a function of curing temperature. The sol-gel is a versatile tool to create transparent metal oxide films that adhere well to various substrates. Therefore, a higher curing temperature might help the condensation reaction of the sol-gel and was approved as shown in Figure 4. It can be seen that when a higher curing temperature was employed, a better UPF was achieved. As control, the UPF has changed slightly after a dip-pad process without curing. With the aid

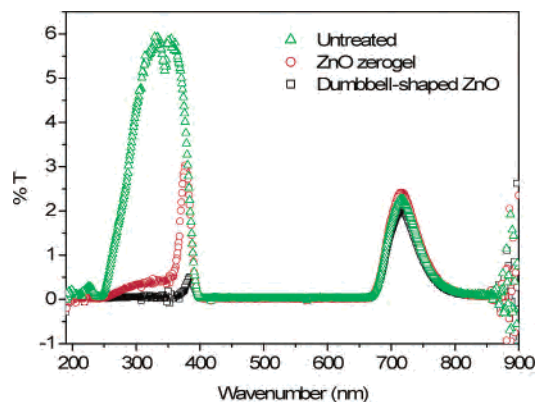


**Figure 5.** UV-vis spectra of cotton fabric sample, treated fabric using ZnO zerogel, and dumbbell-shaped ZnO after 6 h.

of a curing process, the increment seemed approximately expressible by an exponential function. The UPF of more than 400 has been achieved when the curing temperature of at least 150 °C was employed and the UV-blocking range is 352–280 nm. The washfastness was performed according to the AATCC Test Method 61-1996 test No. 2A. The constant UPF was measured after cyclic experiments, and therefore ZnO nanosol has potential application in clothing and textiles. In our previous work, the SPF activity of ZnO nanorods has been evaluated, and an extended UV-blocking range of 375–280 nm was achieved with the UPF of more than 700 after 0.5 h growth of ZnO nanorods.<sup>13a</sup> In Figure 5, the cotton fabric treated using dumbbell-shaped ZnO revealed a high UPF of more than 800; in the visible region, the transmission of the treated substrate was about 10% lower than that of the cotton fabric sample and implied a transparent finishing process. As for the UV range, complete blocking (400–280 nm) was observed, and therefore dumbbell-shaped ZnO presented a higher SPF activity than that of ZnO nanorods<sup>13a</sup> and anatase titania film-treated cellulosic fabrics (the complete UV-blocking range was 332–280 nm<sup>15</sup>). The washfastness of the materials was not presented here. These materials might be applied to some reinforced SPF fields, for example, screens, curtains, window blinds, awnings, and outdoor shelters. The mechanism of the SPF activity is attributed to the electronic structure of semiconductors. The as-prepared products can absorb light with energy of  $h\nu$  that matches or exceeds their band gap energy ( $E_g$ ). The  $E_g$  of ZnO lies in the UV range of the solar spectrum, and therefore dumbbell-shaped ZnO has potential applications in outdoor shelters.

Figure 6 displays the Raman scattering spectra of various ZnO nanostructures. The first-order phonon frequencies of  $E_2$  and  $E_1$  (Longitudinal optical phonon, LO) of wurtzite ZnO were reported to be 438 and 590  $\text{cm}^{-1}$ , respectively.<sup>17</sup> A unique feature of the ZnO spectrum is that its LO signal is weak, while its two-phonon signal is relatively strong.<sup>17c</sup> The bottom trace shows ZnO nanosols are amorphous besides

(17) (a) Xu, C. X.; Sun, X. W.; Dong, Z. L.; Yu, M. B. *Appl. Phys. Lett.* **2004**, *85*, 3878–3880. (b) Bae, S. Y.; Seo, H. W.; Choi, H. C.; Park, J. H.; Park, J. C. *J. Phys. Chem. B* **2004**, *108*, 12318–12326. (c) Hasuike, N.; Fukumura, H.; Harima, H.; Kisoda, K.; Matsui, H.; Saeki, H.; Tabata, H. *J. Phys.: Condens. Matter* **2004**, *16*, S5807–S5810.

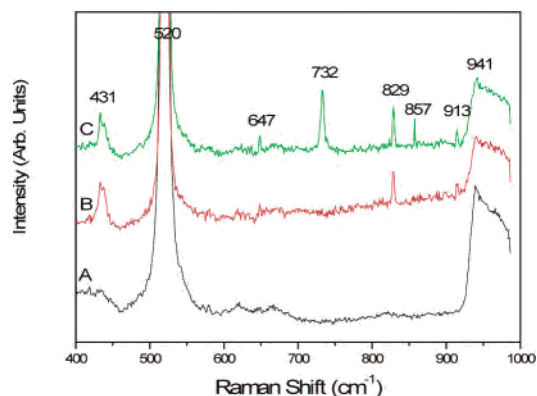


**Figure 6.** Raman scattering spectra of (A) ZnO nanosols, (B) ZnO nanorods, and (C) ZnO dumbbell-shaped crystallites.

the peak at  $520\text{ cm}^{-1}$  and  $941\text{ cm}^{-1}$  originating from silicon substrate. Strong peaks appear at  $431\text{ cm}^{-1}$  and  $829\text{ cm}^{-1}$  which correspond to the wurtzite phase of ZnO (Figure 6A and 6B). Other modes including  $647$ ,  $732$ ,  $857$ , and  $913\text{ cm}^{-1}$  in Figure 6c indicate that the sample is polycrystalline in the sense that it is mainly *c*-axis oriented, but contains small domains with different orientations or consists of crystalline mismatches. The results of XRD and Raman spectrum confirm that the dumbbells are composed of hexagonal ZnO with good crystal quality.

## Conclusions

In summary, our approach toward synthesizing dumbbell-shaped ZnO microcrystallites creates solution-processible homostructures of nanorods under ambient pressure and low temperature and is suitable for industrial preparation. The curing temperature effect on UPF was intensively investigated and revealed that it played an important role during the nanofinishing processes; the higher the curing temper-

ature that was employed, the better the UPF that was achieved. The UPF of more than 400 has been achieved when a curing temperature of at least  $150\text{ }^{\circ}\text{C}$  was employed, and the UV-blocking range is  $352\text{--}280\text{ nm}$ . This finishing process provided a constant washfastness and was suitable for clothing and textiles. The cotton fabric treated using dumbbell-shaped ZnO demonstrated a unique UPF of 800 plus, in the visible region; the transmission of the treated substrate was about 10% lower than that of the cotton fabric sample and implied a transparent finishing process. As for the UV range, complete blocking ( $400\text{--}280\text{ nm}$ ) was observed, and therefore our tentative investigation created a breakthrough to both the ultrahigh UPF and the overall-range of complete UV-radiation blocking. Dumbbell-shaped ZnO presented a wider UV-blocking range than that of ZnO nanosols ( $352\text{--}280\text{ nm}$ ), nanorods ( $375\text{--}280\text{ nm}$ ), and anatase titania films ( $332\text{--}280\text{ nm}$ ). Therefore, the as-prepared structural material demonstrated a significant advance in protective functional treatment and provided a potential commercialization.

**Acknowledgment.** The authors gratefully acknowledge the funding of this study by the The Hong Kong Polytechnic University (HKPolyU Grant No. 4. 14. 56. RGG3) and the Research Grants Council of the Hong Kong SAR Government (RGC Reference: PolyU 5289/03E). We thank HKPolyU Materials Research Center, Materials Characterization & Preparation Facility of The Hong Kong University of Science & Technology (HKUST) for the use of their facilities, and Dr G. K. H. Pang from the Department of Applied Physics of HKPolyU for cooperation in the HRTEM study.

IC0503176